

Droplet-based dielectrophoresis device for on-chip nanomedicine fabrication and improved gene delivery efficiency

Shih-Mo Yang · Hong Yao · Dapeng Zhang ·
Wen Jung Li · Hsiang-Fu Kung · Shih-Chi Chen

Received: 28 May 2014 / Accepted: 3 February 2015 / Published online: 10 February 2015
© Springer-Verlag Berlin Heidelberg 2015

Abstract In this article, we present the design, fabrication, and experimental verification of a droplet-based microfluidic device for effective on-chip fabrication and separation of polymer-based nanoparticles using dielectrophoresis (DEP) effect. The separated polyplexes nanoparticles were used in cells for improved gene transfection efficiency. By adjusting the flow rate of PEI₆₀₀-CyD-FA (H₁) and DNA plasmids, polyplexes products can be mixed and self-assembled inside droplets within approximately a nanoliter volume. This procedure ensures synthesized particles to have a narrow size distribution. In addition, a new microchannel design was developed to automatically coalesce two moving aqueous droplets and to directly extract aqueous polyplex products from oil. Finally, the H₁-DNA polyplexes of ~116 nm diameter were separated via negative DEP force under 8 V_{peak-peak} and 20 MHz conditions

by passing three times through a non-uniform electric field. The biological findings demonstrated that the DEP-treated polyplexes still possessed the ability to enter HUVEC cells and that the gene transfection efficiency was raised to 15 %, as opposed to the control group's 4 % where the polyplexes had no DEP treatment. The quantitative comparison was done by counting the number of cells produced via positive EPFG expression. These hydrodynamic and electrodynamic techniques provide an integrated microfluidic platform for fabricating and screening nanoscale drugs.

Keywords Droplet · Dielectrophoresis · Polymeric nanoparticle · Gene delivery · Particle separation · Lab-on-chip

Abbreviations

<i>H</i>	Height of flow channel
<i>W</i>	Width of flow channel
<i>F</i> _{random}	Random force
<i>F</i> _{deterministic}	Deterministic force
H ₁	Polymer vector, designed for drug/gene delivery
<i>L</i> _{assembling}	Length of assembling channel
<i>Q</i> _{blue}	Volume flow rate of blue liquid
<i>Q</i> _{oil}	Volume flow rate of mineral oil
<i>Q</i> _{red}	Volume flow rate of red liquid
<i>V</i> _{droplet}	Droplet velocity
<i>V</i> _{pp}	Peak-to-peak voltage
FA	Folic acid
CyD	Cyclodextrins
DEP	Dielectrophoresis
PEI	Polyethylenimine
PCR	Polymerase chain reaction
EGFP	Enhanced green fluorescent protein
HUVEC	Human umbilical vein endothelial cell

Shih-Mo Yang and Hong Yao have contributed equally to this work.

S.-M. Yang · H. Yao · D. Zhang · S.-C. Chen (✉)
Department of Mechanical and Automation Engineering
and Shun Hing Institute of Advanced Engineering,
The Chinese University of Hong Kong, Shatin, Hong Kong
e-mail: scchen@mae.cuhk.edu.hk

S.-M. Yang
School of Mechanical and Power Engineering, East China
University of Science and Technology, Shanghai, China

H. Yao · H.-F. Kung
Department of Surgery, School of Biomedical Science
and Stanley Ho Centre for Emerging Infectious Diseases,
The Chinese University of Hong Kong, Shatin, Hong Kong

W. J. Li
Department of Mechanical and Biomedical Engineering,
City University of Hong Kong, Kowloon Tong, Hong Kong

1 Introduction

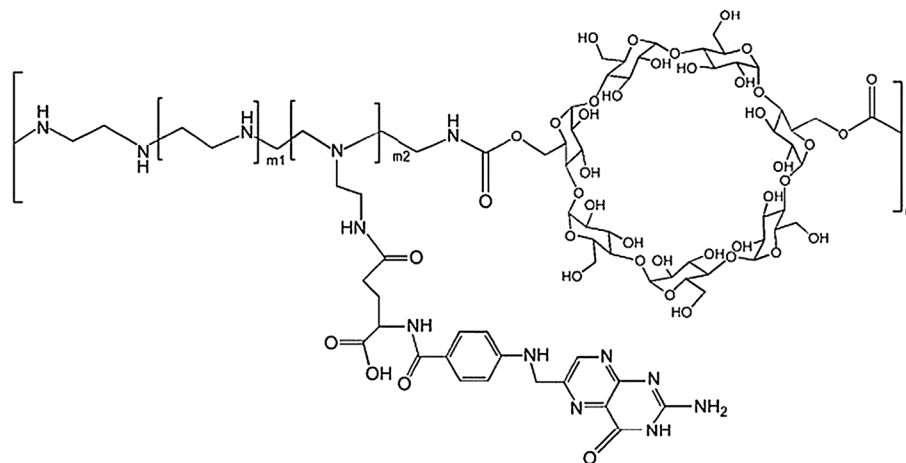
Gene therapy, defined as the treatment of human disease by transferring genetic material into specific cells of the patient, has been researched extensively over the past two decades (Mulligan 1993; Pack et al. 2005). It has been used to treat numerous illnesses, e.g. cardiovascular (Williams and Kingston 2011; Dzau et al. 2003), neurological (Simonato et al. 2013; Burton et al. 2003), cancer and various infectious diseases by delivering specific genes to promote protein synthesis so as to modify existing gene expression and produce pro-drug-activating enzymes and cytotoxic proteins to kill tumour cells (Bunnell and Morgan 1998; Vile et al. 2000). However, its practical applications in a clinical setting are still limited due to many safety considerations and the lack of efficient gene delivery methods (Pack et al. 2005; Liu and Muruve 2003; Lehrman 1999). The design of the gene structure to be delivered, and more importantly, the gene delivery vehicles, together will determine the effectiveness of the gene therapy.

Previously, our group reported a PEI-based polymer vector, named H_1 , which is composed of low molecular weight PEI (600 Da), cross-linked with CyD molecules and folic acid, PEI₆₀₀-CyD-FA. H_1 is a promising biodegradable polymer vector for gene delivery that exhibits high transfection efficiency and low cytotoxicity in various tumour cell lines. (Yao et al. 2009). The structure of H_1 is shown in Fig. 1. (Note that a vector is a gene delivery vehicle that many different DNA drugs can be attached to for treating various diseases.) Traditionally, polyplex nanoparticles (H_1 + DNA) are prepared manually—a time-consuming procedure without precise process control. Added to this, the complex particles structure (Fig. 1) and the nature of the polymer-based products all lead to a lack of uniform size distribution of nanoparticles. Common polymeric nanoparticle size distribution is around 50–1,000 nm with traditional biological synthesis procedures.

To enhance the overall performance of H_1 , we developed a microfluidic device to improve nanoparticle uniformity by on-chip fabrication and sorting. This is because particle size plays a critical role in treating various tumour types and in enhancing the stability of nanoparticles by preventing aggregation and reducing the toxicity level (Merdan et al. 2002; Midoux et al. 2008). For example, liver tumour endothelial cells have a membrane gap of approximately 100 nm, but that of pancreatic tumour cells is only 40 nm. The gap distances between tight endothelial junctions of normal/healthy cells are on the order of 5–10 nm (Rubin and Casarett 1996; Shubik 1982). For liver tumour, nanoparticles of 100 nm in size leak from the tumour vessel, but not from normal vessels. Therefore, nanoparticles leaking from the blood vessels may have extended retention time in the tumour interstition. This feature is termed “the enhanced permeability and retention effect”, which favours tumour interstitial drug accumulation (Sledge and Miller 2003). To date, there have been few effective approaches reported in the literature for precisely controlling the sizes of polymeric nanoparticles for cancer-targeting treatment.

The microfluidic platform, due to its excellent control and manipulating capability for liquid and particles at the microscale, has been the favoured method for chemical and biological applications in recent years (Mark et al. 2010). Among many microfluidic techniques, droplet-based microfluidics and the dielectrophoresis (DEP) phenomena have the potential to separate specific nanoparticle sizes to increase gene delivery efficiency. Droplet-based microfluidics generates discrete volumes via the use of immiscible fluid components (Song et al. 2003). In general, aqueous reagents are injected as discrete droplets, encapsulated by a carrier fluid that wets the microchannel. Droplet methods offer the advantages of improved mixing efficiency and reduced reagent dispersion, and well-controlled concentrations of reagents. These features do not manifest easily in continuous flow-based microfluidics, where fluid mixing

Fig. 1 Structure of PEI₆₀₀-CyD-FA (H_1) (Yao et al. 2009)



is limited by diffusion (Hung et al. 2006; Duraiswamy and Khan 2009). Numerous review articles have been published on the subject of synthesis of polymer particles within microdroplet, including Janus particles, porous particles, microgels, vesicles, nanocrystals, and protein crystals (Song et al. 2006; Park et al. 2010; Wang et al. 2011; Teh et al. 2008). Because of the advantages of its high throughput, we employed a droplet-based platform to mix and assemble polymer-based nanoparticles (H_1) and DNA plasmids in this work.

Dielectrophoresis is an active technique commonly used in microfluidic systems to manipulate and screen micro/nanoparticles (Kuzyk 2011; Çetin and Li 2011; Pethig 2010). Many articles have reported DEP applications, such as particle sorting trapping/assembling (Pommer et al. 2008; Srivastava et al. 2008; Suehiro et al. 2008; Tomkins et al. 2008), and purification for organic and inorganic samples in a broad range of environmental (Chen et al. 2006; Liu et al. 2006), biological and clinical applications (Kuzyk 2011; Çetin and Li 2011; Pethig 2010). As an active manipulating method, DEP has the potential to be applied in separating polymer-based nanoparticles composed of H_1 and DNA plasmids.

In this article, we report a droplet-based microfluidic platform with integrated DEP electrodes for fabricating and sorting polymer-based nanoparticles. Our new microfluidic system integrates the functions of droplet formation and oil/droplet separation in order to extract products directly; the drug delivery vehicle (H_1) and DNA plasmids were assembled in droplets of nanoliter volumes. Metal electrodes were fabricated and integrated in the path of moving drug products inside the microfluidic channel to generate a non-uniform electric field for collecting nanoparticles of specific sizes. In the end, the fluorescence images of HUVEC cells proved that the DEP-treated drug polyplexes not only maintain the functions of gene transfection capability but also generate higher transfection efficiency than the reference sample. In these experiments, we have shown that the microfluidic devices can be a reliable platform for fabricating polymer-based nanoparticles for tumour treatment applications.

2 Materials and methods

2.1 Assembling of H_1 and DNA

Our drug delivery vehicles, H_1 , consist of PEI₆₀₀-CyD and folate. The details of the synthesis and fabrication procedure of H_1 can be found in Yao et al. (2009) and Tang et al. (2006). Here, we describe how H_1 and DNA are prepared and assembled: first, DNA encoded with the enhanced green fluorescent protein (EGFP) was obtained through polymerase chain reaction (PCR) using the pEGFP-N1

plasmid (BD Biosciences, San Jose, CA, USA) as templates. The sequences of the PCR products were confirmed by DNA sequencing. The pEGFP plasmid was transformed into competent DH5 cells, propagated in LB broth supplemented with 100 μ g/mL ampicillin and purified with PureLink™ Hipure Plasmid Maxiprep kit (Invitrogen). The quantity and quality of the purified plasmid DNA were assessed by measuring its optical density at 260–280 nm.

Various N/P ratios (N is the amount of nitrogen in PEI and P is the amount of phosphate in 1 mg DNA) and polyplex diameters were obtained in the packaged droplets by tuning the flow rate and reagent concentration, respectively. After optimization, N/P ratio of 20:1 with a final DNA concentration of 10 μ g/mL was used for later experiments in this work. The hydrodynamic particle size and zeta potentials of the polyplexes were measured at 25 °C by dynamic light scattering using Zetasizer 3000 (Malvern Instruments, Worcestershire, UK) (Yao et al. 2009).

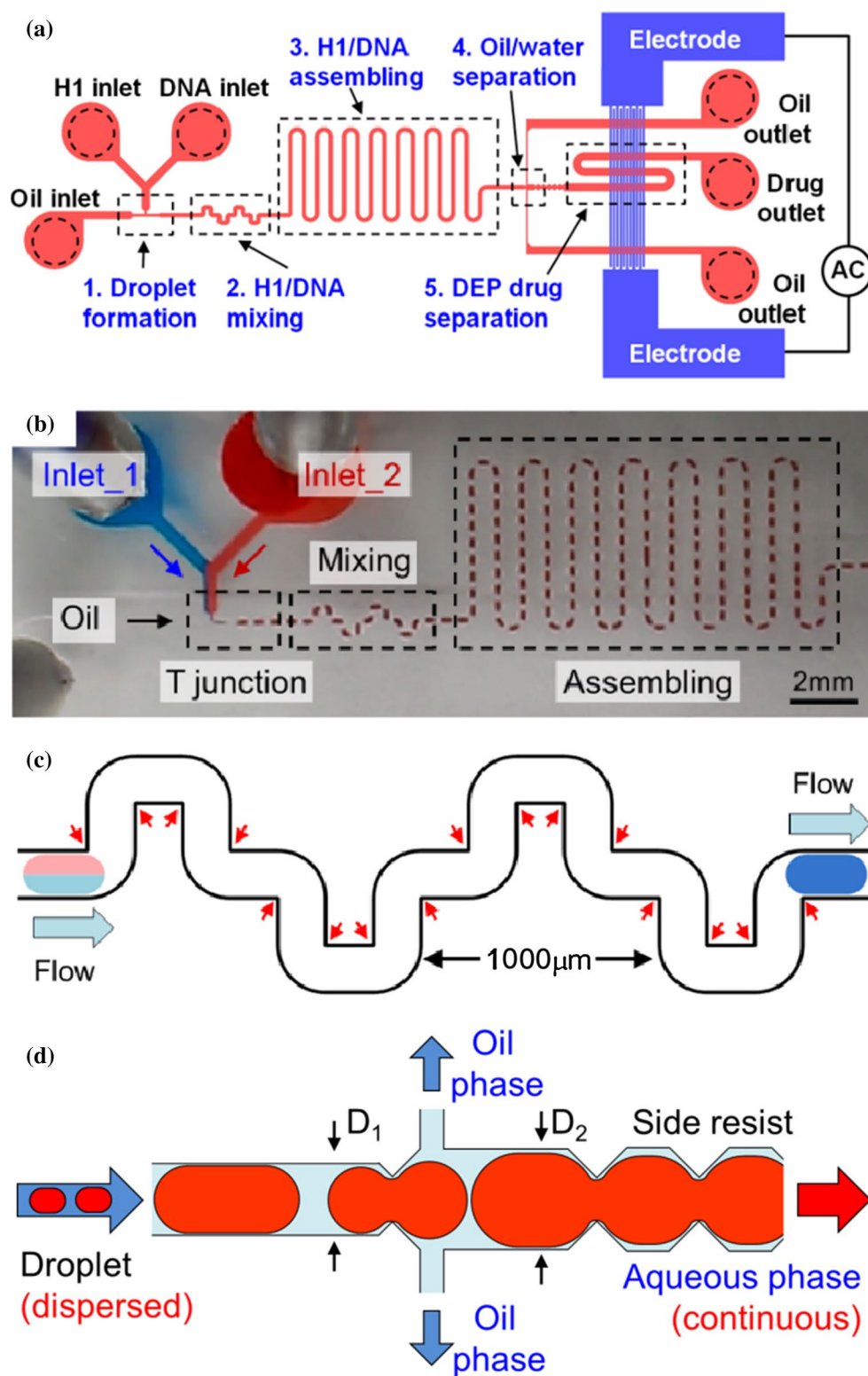
2.2 Droplet-based system

Based on the lab-on-a-chip concept, we developed a microfluidic device that automates five critical steps in the nanoparticle fabrication process: (1) formation of H_1 and DNA droplets, (2) H_1 and DNA mixing, (3) H_1 and DNA self-assembling, (4) H_1 -DNA product extraction, i.e. oil/water separation, and (5) DEP selection for specific particle sizes. Figure 2a shows the schematic of the microfluidic device, where regions labelled from 1 to 5 (with the dash-line) correspond to steps 1–5 described above, respectively. In all experiments, syringe pumps were used to inject the samples, i.e. H_1 , DNA and oil, to the microfluidic device.

We first packaged H_1 and DNA into a droplet for better mixing and assembling as opposed to the conventional off-chip method. In our design, the T-junction configuration was adopted and optimized to generate steady droplets (Seemann et al. 2012; Garstecki et al. 2006). As shown in Fig. 2b, the droplet formation process was demonstrated with blue and red dye, whereas in real experiments, the reagents of H_1 and DNA were transparent. The relative quantities of H_1 and DNA inside the droplet were controlled by adjusting the flow rates from inlet 1 and inlet 2. Mineral oil (M5904, Sigma-Aldrich) with 5 % v/v Span 80 surfactant was continuously injected from the left of the T-junction to separate the aqueous flow from the upper channel and to package H_1 and DNA reagents into a nanoliter scale slug.

To induce and accelerate mixing for the reagents (H_1 and DNA) packaged in the moving droplet in a low Reynolds number flow field, a total of sixteen right-angled turns in the microchannel were designed, Fig. 2c. By this method, H_1 and DNA reagents packaged inside the droplet could be mixed rapidly by shear-induced local vortices in a short distance of travel.

Fig. 2 **a** Schematic diagram of the microfluidic chip integrated with droplet-based microfluidic channels and DEP traps via interdigitated metal electrodes. *Five regions* serve different functions: droplet formation, H₁ and DNA mixing and assembling, product extraction, and particle separation. **b** Image of the droplet generator, reagent mixing, and nanoparticles assembly region on the device. **c** Sixteen right-angled corners, indicated by *red arrows*, were designed to generate chaotic advection for rapid reagent mixing. **d** Schematic diagram of the passive droplet-oil separator. The expanding channel width and a series of triangular structures assist in reducing the droplet velocity and effective droplet merging. The oil component is automatically expelled to the side microchannels by the compression of two converging droplet surfaces



After proper mixing, the H₁ and DNA still need time to self-assemble themselves as effective nanomedicine. Accordingly, a “self-assembly” region comprising a long microchannel, $L_{\text{assembling}}$, was introduced after the reagent mixing region, Fig. 2b. The velocity of the moving droplet

can be determined as $V_{\text{droplet}} = (Q_{\text{red}} + Q_{\text{blue}} + Q_{\text{oil}})/WH$, where the numerator was the combined flow rates from the three inlet ports and W and H were the channel width (200 μm) and height (100 μm), respectively. The time, t , needed for a moving droplet to pass

through the self-assembly region can be calculated as $t = L_{\text{assembling}}/V_{\text{droplet}}$. In our design, the flow velocity in this region was approximately 1,000 $\mu\text{m/s}$ and the droplets passed through the assembling region for tens of seconds. Since mixing in a nanoliter sized droplet is more efficient, we significantly reduced the mixing/assembling time to within 1 min with our device. Compared with off-chip method which requires 10 min of assembling time, on-chip design provides a more efficient method to synthesize $\text{H}_1\text{-DNA}$ and the results are in the following section.

A direct method of separating oil and aqueous components into different collecting ports was developed on our integrated chip. More importantly, this design, combining droplet system and DEP operation, avoids sample pollution and consumption as against conventional methods which require static resting of the mixture for several minutes in order to separate oil and water. As to the mineral oil contained between droplets, we can separate it in a passive way by taking the following two steps: (1) slow down the velocity of the first droplet and (2) remove the oil between the previous and the next droplet. Figure 2d shows the schematic diagram of this passive separation process, where the expanding channel widths ($D_1 = 200 \mu\text{m}$; $D_2 = 280 \mu\text{m}$) assist in slowing down and merging the droplets. The triangular flow-restriction structures further ensure effective merging by repeated flow acceleration and deceleration. When two droplets make contact, the oil is compressed between the surfaces and is forced into the side channels. Accordingly, only the aqueous component product is left to be transported to the DEP separation region downstream and then collected at the drug outlet port.

2.3 DEP operation

A nanoparticle moving in a microfluidic channel experiences random force (F_{random}) and deterministic force ($F_{\text{deterministic}}$). The random force is due to the Brownian motion which can be observed on any nanoscale particles in steady liquid state. The deterministic force is the sum of the gravitational, hydrodynamic, and dielectrophoretic forces (Green and Morgan 1997). In our design, the DEP force plays a dominant role in separating specific-sized particles than the other two effects. This is later validated in the experiments, where the size distribution of polyplexes before and after DEP treatment is considerably different. During a DEP operation, a non-uniform electric field completely filled the microchannel, where stronger electric fields were located near the bottom electrodes. When the nanomedicine of various sizes flowed through the electrodes, larger particles experienced more positive DEP force and were attracted to the electrode in the bottom of the microchannel, Fig. 3a, b. We used a commercial finite element software, CFD-ACE+ (CFDRC, Huntsville, AL, USA), to

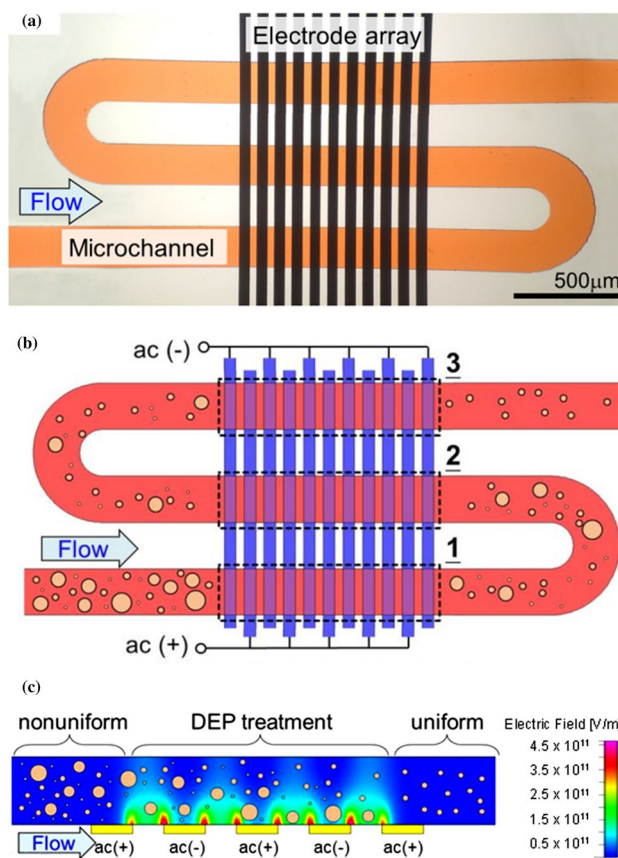


Fig. 3 Design of DEP electrodes for particle separation: **a** image of metal electrodes with a microfluidic channel filled with red dye. **b** Schematic diagram of DEP separation. Nanoparticles are driven by fluidic forces and passed three times through the DEP working regions, indicated by dotted lines. **c** Side view of the flow channel above the electrodes, plotted with the non-uniform AC electric field. Note that the polyplexes of larger sizes are attracted to the bottom electrodes

simulate the steady-state electric field. Figure 3c shows the simulated results for the root mean square of an AC electric field (E^2) distribution inside the microchannel. The nanomedicine with negative DEP force passed through the electrodes and was collected at the outlet port for the next step of drug delivery efficiency testing.

3 Results and discussion

3.1 Control of concentration in droplets

In this work, the flow rate ratio of aqueous liquid to oil, $R = (Q_{\text{red}} + Q_{\text{blue}})/Q_{\text{oil}}$, controlled the properties of droplet formation. For example, when $R = 2$ with the constant oil flow rate of $Q_{\text{oil}} = 5 \text{ nL/s}$, the length of droplet was around 1,500 μm . As the value of R increased to 3 and 4, the droplet length reduced to 620 and 420 μm , respectively. These

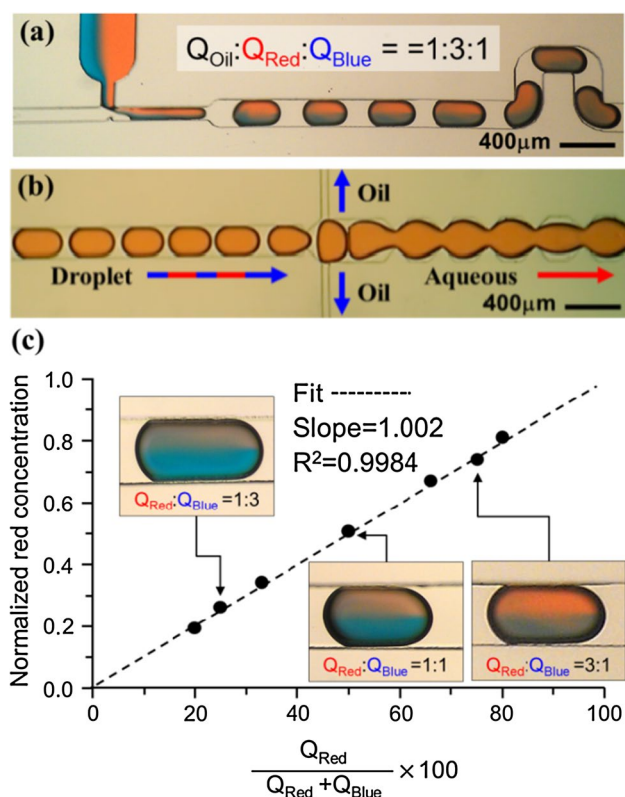


Fig. 4 **a** Packaging of two reagents into various droplet volumes was achieved by adjusting the flow rates of aqueous and oil components in the T-junction design. The droplet-based device provided an effective method of mixing the drug delivery vehicle (H_1) and DNA within a nanoliter volume. **b** Oil expulsion and aqueous coalescing in the microchannel with properly sized droplets and droplet distances. The polyplex products can be directly collected at the output port. The scale bar is $400\mu m$. **c** A plot illustrating red concentration inside a constant droplet volume with different red/blue flow rates. The analysis demonstrated that on-chip droplet-based mixing of H_1 and DNA reagents, adjusted by the pumping velocity, was reliable when the flow rate fell between 0.5 and 20 nL/s. The channel width was $200\mu m$

results demonstrated that the droplet volume can be controlled by adjusting the R value or the flow rates of red and blue dyes and oil, Fig. 4a.

For packaging different mixing ratios of reagents in identical droplet volumes, the total flow rate of the red and blue streams was kept constant by changing the ratio of Q_{red} to Q_{blue} under fixed R value condition. Figure 4c shows the relationship between the red concentration and red/blue dye ratio, $Q_{red}/(Q_{red} + Q_{blue})$. The normalized red concentration in a constant droplet volume was found proportional to the red dye flow rate, i.e. Q_{red} , by analysing the proportion of red in a single mixed droplet. This result is important as it indicates that our chip can control reagent mixing ratios by tuning the flow rates of the injected liquids. In other words, by adjusting the ratio of H_1 and DNA, we can produce different polyplexes according to

appropriate N/P ratios. Conventional methods of producing polyplexes involved preparing initial concentrations of H_1 and DNA and mixing them in Eppendorf. Often, they produce polyplexes with a wide size distribution. The technique of the on-chip droplet generator can significantly simplify the preparation of complex reagents for synthesizing polyplexes as it precisely controls the droplet volume and packages reagents in different ratios by simply tuning the flow rate of the injected aqueous components. Due to the precise mixing ratio and effective mixing in small droplets, we expect the resulting polyplexes to have a more uniform size distribution (experimental results are in the next section).

Figure 4b illustrates the separation mechanism of oil and aqueous components, using internal geometry designed to slow and coalesce moving droplets as well as to expel oil. Based on our experiments and observation, a better separation of oil and aqueous component can be achieved when the droplet length falls between 1.5 and 2 times the channel width.

3.2 Determination of polyplexes size distribution

To validate the effectiveness of the droplet-based DEP microdevice, we examine the size distributions of polyplexes under three conditions: (1) manual mixing in Eppendorf, (2) mixing in droplets (on-chip) without DEP, and (3) mixing in droplets with DEP. The size distribution of nanoparticles was characterized by the DelsaTM Nano, which utilizes photon correlation spectroscopy to determine particle size in a fluid, as shown in Fig. 5a–c.

For the control group, (i.e. manual mixing), 1 c.c. of H_1 and 1 c.c. of DNA solution were mixed in Eppendorf, followed by 10 min of static resting for particles assembling, shown in Fig. 5a. For the on-chip method without DEP, the H_1 and DNA solutions were injected from the inlet ports for self-assembly with a processing time of 1 min, shown in Fig. 5b. Comparing Fig. 5a and b, the results show that the size of polyplexes assembled in nanoliter volume had a narrower distribution. The peak polyplex diameters in the control group and droplet-based device group were 185.9 and 137.2 nm, respectively. These results showed that the mixing efficiency of our droplet-based platform in nanoscale volumes is high (ten times faster) and that the products are more uniform.

Under condition (3), $8V_{pp}$ at 20 MHz was applied to the electrodes for DEP treatment in the bottom of the microchannel after the polyplexes passed through the water–oil separation region. (The DEP parameters were experimentally determined to allow best cell transfection efficiency, discussed in Sects. 3.3 and 3.4.) Polyplexes polarized by positive DEP effect were then attracted to the glass substrate, where the electric field was strong. Nanoparticles

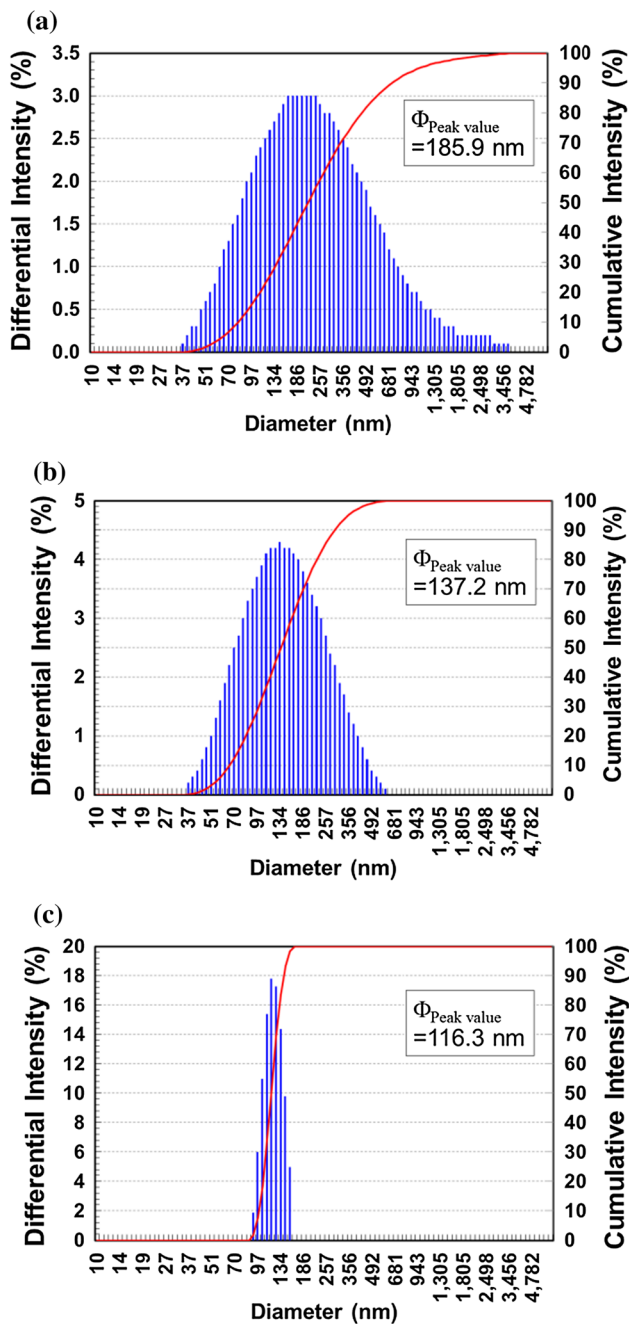


Fig. 5 Size distribution for H_1 -DNA polyplexes: **a** manual mixing in Eppendorf. **b** On-chip mixing in droplets without DEP. **c** On-chip mixing in droplets with DEP. The results suggest droplet-based method produces more uniform polyplexes and DEP may be used for precise nanomedicine fabrication

that experienced negative DEP force passed through three DEP regions and were collected at the outlet port. The results of the DEP treatment are plotted in Fig. 5c, showing an even narrower size distribution that peaked around 116.3 nm and the majority of the larger particles was effectively trapped by the electrodes.

It is worth to note that, in Fig. 5c, polyplexes with a size less than ~80 nm were also removed by the DEP treatment. We believe the small polyplexes were trapped to the electrodes due to the surface charges they carried (since DNA is negatively charged). In other words, for small polyplexes, the electrostatic forces become dominant over the drag force in flow. Since the charges on the polyplexes were difficult to quantify, we did not include them in our simulations in Sect. 2.3.

3.3 Transfection ability after DEP treatment

Experiments were devised to verify and quantify the level of enhancement for gene transfection with DEP-treated H_1 -DNA polyplexes. First, we need to validate that the polyplexes still possess the ability to enter cells for gene transfection. A direct method to verify this is to identify the locations of the fluorescence labelled particles inside a HUVEC cell. Figure 6 presents three images obtained from a custom-developed confocal system (Zhang et al. 2013), where the blue region shows the cell body and the green dots indicate the locations of the polyplexes. These images were obtained through a serial top-down z-scanning process and reconstructed using ImageJ. The result validates that the polyplexes had entered the HUVEC cell after 8 h of interaction.

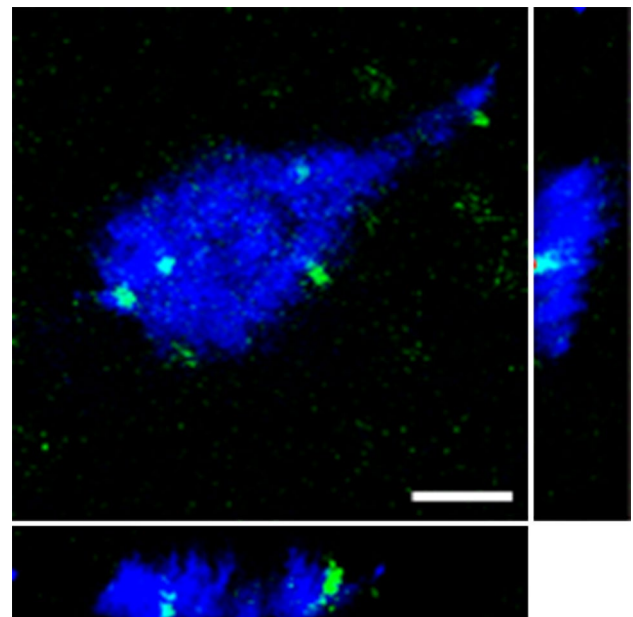


Fig. 6 Confocal cross-sectional images of the HUVEC cell. The blue region represents HUVEC cell, and the green dots indicate the locations of DEP-treated polyplexes. These images verified that the DEP-treated polyplexes still have the gene transfection ability. The scale bar is 10 μ m

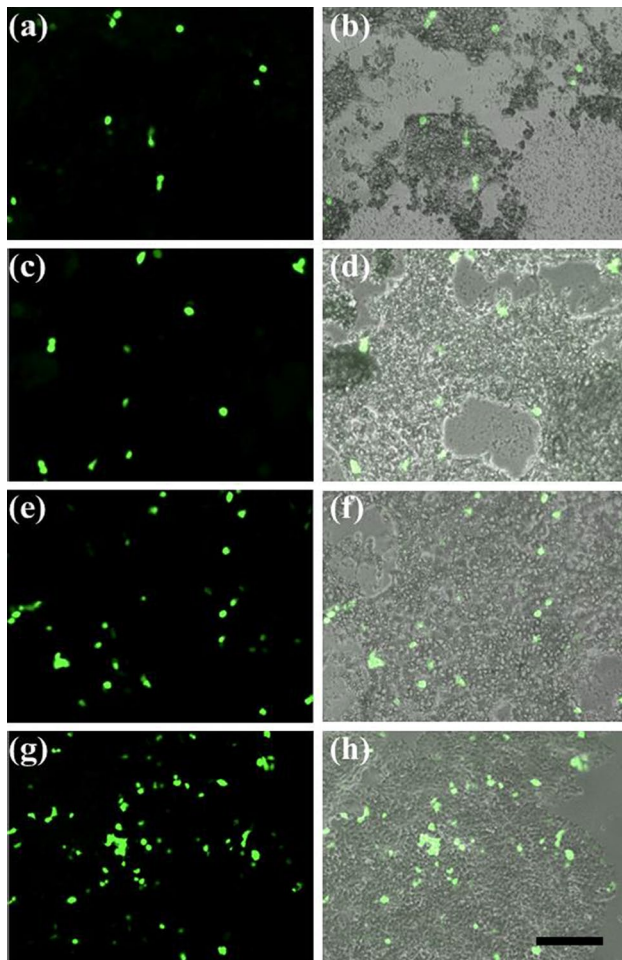


Fig. 7 Cell count of positive EGFP expression showed that the transfection efficiency of DEP-treated polyplexes was significantly increased: **a, b** 24-h control group, **c, d** 48-h control group, **e, f** 24-h DEP-treated group, **g, h** 48-h DEP-treated group, **b, d, f, h** were merged images of fluorescent and bright field images. The transfection percentages of DEP-treated and non-DEP-treated polyplexes in HUVEC cells were 15 and 4 %, respectively. The scale bar is 200 μm

3.4 Transfection efficiency on HUVEC cells

Enhanced green fluorescent protein (EGFP) expression analysis was used to evaluate the transfection efficiency *in vitro*. Specifically, we examined the transfection efficiency of H_1 in HUVEC cells and the percentage of EGFP positive cells was counted over ten randomly selected fields. HUVEC cell was chosen for the experiment as it typically has low cell transfection efficiency. After DEP treatment, large polymer particles were removed, and nanoparticles sized around 116.3 nm were collected in the outlet of chip. In order to compare the drug effect between the control group (off-chip synthesis without DEP treatment) and our on-chip droplet-based method with DEP treatment, the collected polyplexes concentration was both adjusted to

the same N/P ratio level, and the culture medium was both replaced at 37 °C. After a 4-h cell culture, the transfection medium was replaced with fresh growth medium and incubated in two batches for 24 and 48 h, respectively. Figure 7 shows four representative positive EGFP expression images of the DEP-treated cells and those of the control group after 24- and 48-h incubation. When the cells were cultured for 48 h, the percentage of EGFP positive cells in the DEP-treated polyplexes and the control group were approximately 15 and 4 %, respectively. We found that, compared with the polyplexes obtained via conventional protocol, the DEP-treated H_1 had superior transfection ability. Such distinction shows that the transfection efficiency of polyplexes is improved by a factor of 3.8 times after the DEP treatment. Note that since larger polyplexes in the control group cannot enter the cells, it is expected that the DEP-treated H_1 would result in better transfection efficiency at the same concentration level. In addition, larger polyplexes mean a DNA can be simultaneously bound to multiple polymer vectors, which prevents the DNA to be effectively released from the vector carrier (H_1). As a result, larger polyplexes, even when they enter the cells, will generate less effect than small polyplexes. This experiment indirectly validated that the smaller-sized polyplexes were effectively collected after the DEP treatment. The biological results strongly indicate that our microfluidic design and the concept of DEP particle sorting have potential applications in gene therapy and nanomedicine fabrication. Note that all results reported in this article have been repeated many times over a period of 2 years with various DEP processing parameters, proving the good reproducibility of the droplet-based platform.

4 Conclusions

In this work, we demonstrated the integration of a droplet-based platform and DEP treatment for the fabrication of H_1 -DNA polyplexes, a kind of nanomedicine for tumour-targeted gene therapy. The droplet-based platform realizes the concept of “lab-on-a-chip” by performing multiple time-consuming laboratory tasks in one single chip with significantly improved transfection efficiency (15 vs. 4 %) and reduced time (1 vs. 10 min). These functions, including droplet formation, mixing, self-assembling, extraction, and particle sorting, are all integrated on a single chip with sub-sections to perform individual functions. The device is made by PDMS microchannels bonded to a glass slide with patterned DEP metal electrodes. The experimental results verified that our microdevice can effectively fabricate nanoscale polymer-based particles (H_1 -DNA) for improved gene transfection. The resulting nanomedicine is used to treat and study mice with hepatocellular carcinoma and will be reported in a separate article. We expect improved drug

efficacy and reduced toxicity in the animal experiments due to the precisely controlled particle sizes.

Acknowledgments This research is supported by project #BME-p3-12 of the Shun Shing Institute of Advanced Engineering, The Chinese University of Hong Kong.

References

- Bunnell BA, Morgan RA (1998) Gene therapy for infectious diseases. *Clin Microbiol Rev* 11(1):42–56
- Burton EA, Glorioso JC, Fink DJ (2003) Gene therapy progress and prospects: parkinson's disease. *Gene Ther* 10(20):1721–1727
- Çetin B, Li D (2011) Dielectrophoresis in microfluidics technology. *Electrophoresis* 32(18):2410–2427
- Chen Z, Wu Z, Tong L, Pan H, Liu Z (2006) Simultaneous dielectrophoretic separation and assembly of single-walled carbon nanotubes on multigap nanoelectrodes and their thermal sensing properties. *Anal Chem* 78(23):8069–8075
- Duraiswamy S, Khan SA (2009) Droplet-based microfluidic synthesis of anisotropic metal nanocrystals. *Small* 5(24):2828–2834
- Dzau VJ, Beatt K, Pompilio G, Smith K (2003) Current perceptions of cardiovascular gene therapy. *Am J Cardiol* 92(9):18–23
- Garstecki P, Fuerstman MJ, Stone HA, Whitesides GM (2006) Formation of droplets and bubbles in a microfluidic T-junction—scaling and mechanism of break-up. *Lab Chip* 6(3):437–446
- Green NG, Morgan H (1997) Dielectrophoretic separation of nanoparticles. *J Phys D Appl Phys* 30(11):L41
- Hung LH, Choi KM, Tseng WY, Tan YC, Shea KJ, Lee AP (2006) Alternating droplet generation and controlled dynamic droplet fusion in microfluidic device for CdS nanoparticle synthesis. *Lab Chip* 6(2):174–178
- Kuzyk A (2011) Dielectrophoresis at the nanoscale. *Electrophoresis* 32(17):2307–2313
- Lehman S (1999) Virus treatment questioned after gene therapy death. *Nature* 401(6753):517–518
- Liu Q, Muruve DA (2003) Molecular basis of the inflammatory response to adenovirus vectors. *Gene Ther* 10(11):935–940
- Liu X, Spencer JL, Kaiser AB, Arnold WM (2006) Selective purification of multiwalled carbon nanotubes by dielectrophoresis within a large array. *Curr Appl Phys* 6(3):427–431
- Mark D, Haeberle S, Roth G, von Stetten F, Zengerle R (2010) Microfluidic lab-on-a-chip platforms: requirements, characteristics and applications. *Chem Soc Rev* 39(3):1153–1182
- Merdan T, Kopeček J, Kissel T (2002) Prospects for cationic polymers in gene and oligonucleotide therapy against cancer. *Adv Drug Deliv Rev* 54(5):715–758
- Midoux P, Breuzard G, Gomez JP, Pichon C (2008) Polymer-based gene delivery: a current review on the uptake and intracellular trafficking of polyplexes. *Curr Gene Ther* 8(5):335–352
- Mulligan R (1993) The basic science of gene therapy. *Science* 260(5110):926–932
- Pack DW, Hoffman AS, Pun S, Stayton PS (2005) Design and development of polymers for gene delivery. *Nat Rev Drug Discov* 4(7):581–593
- Park JI, Saffari A, Kumar S, Günther A, Kumacheva E (2010) Microfluidic synthesis of polymer and inorganic particulate materials. *Annu Rev Mater Res* 40(1):415–443
- Pethig R (2010) Review article—dielectrophoresis: status of the theory, technology and applications. *Biomicrofluidics* 4(2):022811–022835
- Pommer MS, Zhang Y, Keerthi N, Chen D, Thomson JA, Meinhart CD, Soh HT (2008) Dielectrophoretic separation of platelets from diluted whole blood in microfluidic channels. *Electrophoresis* 29(6):1213–1218
- Rubin P, Casarett G (1996) Microcirculation of tumours part I: anatomy, function and necrosis. *Clin Radiol* 17(3):220–229
- Seemann R, Brinkmann M, Pfohl T, Herminghaus S (2012) Droplet based microfluidics. *Rep Prog Phys* 75(1):016601
- Shubik P (1982) Vascularization of tumours: a review. *J Cancer Res Clin Oncol* 103(3):211–226
- Simonato M, Bennett J, Boulis NM, Castro MG, Fink DJ, Goins WF, Glorioso JC (2013) Progress in gene therapy for neurological disorders. *Nat Rev Neurol* 9(5):277–291
- Sledge GW, Miller KD (2003) Exploiting the hallmarks of cancer: the future conquest of breast cancer. *Eur J Cancer* 39(12):1668–1675
- Song H, Tice JD, Ismagilov RF (2003) A microfluidic system for controlling reaction networks in time. *Angew Chem Int Ed* 42(7):768–772
- Song H, Chen DL, Ismagilov RF (2006) Reactions in droplets in microfluidic channels. *Angew Chem Int Ed* 45(44):7336–7356
- Srivastava SK, Daggolu PR, Burgess SC, Minerick AR (2008) Dielectrophoretic characterization of erythrocytes: positive ABO blood types. *Electrophoresis* 29(24):5033–5046
- Suehiro J, Ikeda N, Ohtsubo A, Imasaka K (2008) Fabrication of bio/nano interfaces between biological cells and carbon nanotubes using dielectrophoresis. *Microfluid Nanofluid* 5(6):741–747
- Tang GP, Guo HY, Alexis F, Wang X, Zeng S, Lim TM, Wang S (2006) Low molecular weight polyethylenimines linked by β -cyclodextrin for gene transfer into the nervous system. *J Gene Med* 8(6):736–744
- Teh SY, Lin R, Hung LH, Lee AP (2008) Droplet microfluidics. *Lab Chip* 8(2):198–220
- Tomkins MR, Wood JA, Docoslis A (2008) Observations and analysis of electrokinetically driven particle trapping in planar microelectrode arrays. *Can J Chem Eng* 86(4):609–621
- Vile RG, Russell SJ, Lemoine NR (2000) Cancer gene therapy: hard lessons and new courses. *Gene Ther* 7(1):2–8
- Wang JT, Wang J, Han JJ (2011) Fabrication of advanced particles and particle-based materials assisted by droplet-based microfluidics. *Small* 7(13):1728–1754
- Williams PD, Kingston PA (2011) Plasmid-mediated gene therapy for cardiovascular disease. *Cardiovasc Res* 91(4):565–576
- Yao H, Ng SS, Tucker WO, Tsang YKT, Man K, Wang XM, Lin MC (2009) The gene transfection efficiency of a folate-PEI₆₀₀-cyclodextrin nanopolymer. *Biomaterials* 30(29):5793–5803
- Zhang D, Cheng J, Chen SC (2013) Multi-depth real-time confocal imaging. In: Proceedings of the international symposium on optomechatronic technologies (ISOT)